Transient electronic dynamics of noninteracting open systems beyond linear response

To cite this article: Yan Mo *et al* 2009 *J. Phys.: Condens. Matter* **21** 355301

View the article online for updates and enhancements.

Transient electronic dynamics of noninteracting open systems beyond linear response

Yan Mo[1,2]**, Xiao Zheng**[1]**, GuanHua Chen**[2] **and YiJing Yan**[1]

[1] Department of Chemistry, Hong Kong University of Science and Technology, Kowloon, Hong Kong
[2] Department of Chemistry, The University of Hong Kong, Hong Kong

E-mail: chxzheng@ust.hk

Abstract
We present analytical results on the transient current response of noninteracting open electronic systems under time-dependent external voltages in both linear- and nonlinear-response regimes. The derivations are based on an equation of motion formalism for the system reduced single-electron density matrix (Zheng *et al* 2007 *Phys. Rev.* B **75** 195127). Dissipative interactions between the system and leads are treated by the nonequilibrium Green's function approach. The linear-response dynamics is characterized by the analytical admittance spectrum of the open system, through which the quantum coherent transport properties are mapped to equivalent classical circuits. The nonlinear-response current spectrum not only resolves the intrinsic energetic configuration of the system, but also reflects the unique dynamical features due to the transient characteristics of the applied voltages.

(Some figures in this article are in colour only in the electronic version)

1. Introduction

Investigation on the transient dynamics of open electronic systems is of fundamental significance to the development of nanoelectronics [1–13]. The quantum coherent transport properties of mesoscopic and nanoscopic conductors have been studied extensively [2, 9–11, 14]. Efforts have been made to map the linear-response electronic dynamics to equivalent classical circuits, for the convenience of describing quantum transport properties and designing nanoelectronic devices. For instance, it has been demonstrated both experimentally [11] and theoretically [8–10] that, at low frequency and low temperature, the coherent dynamics of a single-lead quantum dot can be characterized by a serial resistor–capacitor circuit. The quantum features are partially manifested by the circuit parameters. The resistor is associated with the charge relaxation rate, while the capacitor originates from the finite density of states at the system-lead contact [8]. In particular, for a single-channel system at zero temperature, the resistor assumes exactly a value of half a resistance quantum, which is universal and independent of the transmission details [8].

As the voltage amplitude becomes large, high-frequency electronic transition modes are activated. The linear-response theory no longer adequately characterizes the dynamic behavior of the open system, and nonlinear effects need to be explicitly accounted for. Moreover, the admittance and current spectra vary sensitively as the voltage changes its time dependence. Consequently, nonlinear-response dynamics not only resolves the intrinsic system properties, but also reflects the unique features due to the transient characteristics of the applied voltage. These nonlinear features provide additional information that can be used for a more comprehensive diagnosis of the system under study. For instance, it has been demonstrated that the nonlinear-response current spectrum under a step voltage reveals distinctly and faithfully the energetic configuration of an interacting quantum dot [15].

To have a more insightful understanding of the quantum coherent features of open systems, we investigate the dynamic properties of noninteracting model systems. The transient current in response to time-dependent voltage has been addressed by Jauho *et al* in a general framework of nonequilibrium Green's function (NEGF) formalism [16]. In their studies the transport dynamics is initiated from a state

where the open system and leads are completely decoupled before the application of turn-on voltage. In this work we adopt an experimentally more relevant scenario, where a fully coupled composite system is considered, which stays in thermodynamic equilibrium prior to the voltage switch-on. The voltage-driven electronic dynamics has also been solved *numerically* by a formally exact hierarchical equations of motion formalism from the perspective of quantum dissipation theory [15, 17–20]. Intriguing phenomena such as dynamical Coulomb blockade [15] and dynamical Kondo transitions [20] have been revealed for interacting systems. However, *analytical* results are essentially important for a clear physical picture of the underlying mechanisms. In this work, we derive analytical response current spectra for noninteracting open systems. All the derivations are based on an equation of motion (EOM) for the reduced single-electron density matrix (RSDM) of the open system [7]. In the linear-response regime, we analyze in detail the voltage-independent dynamic admittance of the open system. Based on the analytical admittance spectrum obtained, we then propose and evaluate the equivalent classical circuit associated with coherent transport through the system. For electronic dynamics beyond linear response, we focus on the unique features due to the specific time-dependent form of applied voltage. The characteristic single-electron transitions under various types of external voltages are also highlighted. In particular, analytical response current spectra are obtained for step-, delta-, and sinusoidal-function voltages.

The remainder of this paper is organized as follows. In section 2, we derive the general formulae of both the linear- and nonlinear-response current spectrum under externally applied voltages. In section 3, the linear-response dynamic admittance of a two-lead model system and its equivalent classical circuit are presented. In section 4, we exploit the unique features of the transient response current due to the specific time-dependent form of applied voltage. Finally, we conclude in section 5.

2. Response current spectrum

2.1. Linear-response current spectrum

Consider a general case that a noninteracting system is coupled to an arbitrary number of leads. Upon the application of a time-dependent voltage $V_\alpha(t)$ to the lead α, the chemical potential of the lead α varies accordingly, i.e. $\mu_\alpha(t) = \mu_\alpha^{eq} + \Delta_\alpha(t) = \mu_\alpha^{eq} - eV_\alpha(t)$. The equilibrium Fermi energy μ_α^{eq} at each lead is set to zero. The noninteracting system of primary interest is characterized by the reduced single-electron Hamiltonian matrix $h(t)$. Hereafter, a boldface symbol denotes a matrix in a site/level representation of the reduced system. The time-dependent current through the lead α can be evaluated by the Keldysh NEGF formalism as [21, 22]

$$I_\alpha(t) = \frac{e}{\hbar} \int d\tau \ \mathrm{tr}[G^< \Sigma_\alpha^a + G^r \Sigma_\alpha^< + \mathrm{h.c.}]. \quad (1)$$

Here, tr is the matrix trace; $AB \equiv A(t, \tau)B(\tau, t)$ denotes the product of the specified lesser (<), retarded (r) or advanced (a)

Green's function and self-energy matrices in the time domain. Denote also equilibrium quantities by bar symbols, such as $\bar{G}^{s}(t, \tau) = \bar{G}^{s}(t - \tau)$ and $\bar{\Sigma}_\alpha^s(t, \tau) = \bar{\Sigma}_\alpha^s(t - \tau)$, with $s = \mathrm{r, a}$ or <.

In the linear-response regime, where voltages of small amplitudes are applied to the leads, the transient current can be evaluated by

$$
\begin{aligned}
I_\alpha^{(1)}(t) = \frac{e}{\hbar} \int d\tau \ \mathrm{tr}[&\delta G^< \bar{\Sigma}_\alpha^a + \bar{G}^< \delta \Sigma_\alpha^a \\
&+ \delta G^r \bar{\Sigma}_\alpha^< + \bar{G}^r \delta \Sigma_\alpha^< + \mathrm{h.c.}],
\end{aligned} \quad (2)
$$

with the first-order changes of the Green's functions in response to the applied voltages as $\delta G^s(t, \tau) \equiv G^s(t, \tau) - \bar{G}^s(t - \tau)$, and the changes of self-energies as $\delta \Sigma_\alpha^s(t, \tau) \equiv \Sigma_\alpha^s(t, \tau) - \bar{\Sigma}_\alpha^s(t - \tau)$. In particular, $\delta G^{\mathrm{r,a}}(t, \tau)$ are obtained by solving their respective Dyson's equations, by noting that

$$\delta \Sigma_\alpha^s(t, \tau) = \int d\omega \frac{\Delta_\alpha(\omega)}{2\pi\omega} (e^{-i\omega t} - e^{-i\omega \tau}) \bar{\Sigma}_\alpha^s(t - \tau). \quad (3)$$

Here, $\Delta_\alpha(\omega) \equiv \mathcal{F}[\Delta_\alpha(t)]$, where $\mathcal{F}$ stands for the Fourier transform operation.

Presuming a time-independent reduced single-electron Hamiltonian h, equation (2) can be formally simplified (see appendix A for details). The final expression of the response current spectrum, $I_\alpha(\omega) \equiv \mathcal{F}[I_\alpha(t)]$, is

$$I_\alpha^{(1)}(\omega) = \frac{e}{h} \sum_\beta \frac{\Delta_\beta(\omega)}{\omega} \int d\epsilon \ \mathrm{tr}[\mathcal{G}_{\alpha\beta}(\epsilon; \omega)], \quad (4)$$

with $\sum_\beta$ denoting the summation over all coupling leads, and

$$
\begin{aligned}
\mathcal{G}_{\alpha\beta} = \ &\delta_{\alpha\beta}(\bar{G}_+^< \check{\Sigma}_\alpha^a + \bar{G}_+^r \check{\Sigma}_\alpha^< - \check{\Sigma}_\alpha^r \bar{G}^< - \check{\Sigma}_\alpha^< \bar{G}^a) \\
&+ \bar{G}_+^r \check{\Sigma}_\beta^r (\bar{G}^< \bar{\Sigma}_\alpha^a + \bar{G}^r \bar{\Sigma}_\alpha^<) + (\bar{G}_+^< \check{\Sigma}_\beta^a + \bar{G}_+^r \check{\Sigma}_\beta^<) \\
&\times \bar{G}^a \bar{\Sigma}_\alpha^a - (\bar{\Sigma}_\alpha^r \bar{G}^< + \bar{\Sigma}_\alpha^< \bar{G}^a)_+ \check{\Sigma}_\beta^a \bar{G}^a \\
&- (\bar{\Sigma}_\alpha^r \bar{G}^r)_+ (\check{\Sigma}_\beta^r \bar{G}^< + \check{\Sigma}_\beta^< \bar{G}^a).
\end{aligned} \quad (5)
$$

On the right-hand side (rhs) of equation (5), we have adopted the abbreviations $\bar{A}_+ \equiv \bar{A}(\epsilon + \omega)$, $(\bar{A}\bar{B})_+ \equiv \bar{A}_+ \bar{B}_+$ and $\check{A} \equiv \bar{A}(\epsilon) - \bar{A}(\epsilon + \omega)$ for any matrix, or pair of matrices. Apparently, $\mathcal{G}_{\alpha\beta}$ of equation (5) depends only on the equilibrium Green's functions and self-energies; so does the current spectrum $I_\alpha^{(1)}(\omega)$ of equation (4), which is also of linear dependence on the applied voltage. $\mathcal{G}_{\alpha\beta}(\epsilon; \omega)$ can be greatly simplified with the wide-band limit (WBL) approximation adopted for the leads [16], i.e. $\check{\Sigma}_\alpha^{\mathrm{r,a}} = 0$, and $\check{\Sigma}_\alpha^<(\epsilon) = i[f_\alpha(\epsilon) - f_\alpha(\epsilon_+)]\Gamma_\alpha$. Here $\epsilon_\pm \equiv \epsilon \pm \omega$, $f_\alpha(\epsilon)$ is the Fermi distribution function for lead α, Γ_α is the linewidth matrix for lead α and $\Gamma \equiv \sum_\alpha \Gamma_\alpha$ is the total linewidth matrix. The WBL approximation has been shown to be valid as long as the variation of applied voltage stays within the range of lead bandwidth [7]. Exact numerical investigations have revealed that the non-WBL effects preserve largely the overall lineshape of the response current spectrum while modifying the amplitude [18]. Under the WBL approximation, equation (5)

leads to

$$\mathcal{G}^{\text{WBL}}_{\alpha\beta} = \delta_{\alpha\beta}(\bar{G}^{\text{r}}_+ \check{\Sigma}^<_\alpha - \check{\Sigma}^<_\alpha \bar{G}^{\text{a}}) + \bar{G}^{\text{r}}_+ \check{\Sigma}^<_\beta \bar{G}^{\text{a}} \bar{\Sigma}^{\text{a}}_\alpha$$
$$- (\bar{\Sigma}^{\text{r}}_\alpha \bar{G}^{\text{r}})_+ \check{\Sigma}^<_\beta \bar{G}^{\text{a}}. \qquad (6)$$

More generally, $h(t)$ varies in time, as the reduced system may be subjected to time-dependent external fields, such as laser pulses or bias/gate voltages. We have thus $h(t) = h_0 + \Delta_{\text{D}}(t)$, with $\Delta_{\text{D}}(t)$ being the field-induced single-electron Hamiltonian. In the linear-response regime, $\Delta_{\text{D}}(t)$ gives an extra contribution to $\delta G^s(t, \tau)$ and hence complicates further the final result for $\mathcal{G}_{\alpha\beta}(\epsilon; \omega)$. The relevant derivations are presented in appendix A. With nonzero $\Delta_{\text{D}}(t)$, displacement current should be explicitly accounted for to recover the conservation of total current [23, 24]. It is important to point out that for realistic systems $\Delta_{\text{D}}(t)$ is to be determined in a self-consistent manner with $G^s(t, \tau)$. In principle, the interaction between the reduced system and external electromagnetic fields that gives rise to $\Delta_{\text{D}}(t)$ is characterized by Maxwell's equations, which need to be solved simultaneously with Dyson's equations for $G^s(t, \tau)$. In practice, a more tractable approach is to adopt a quasi-static approximation and treat the electrostatic interactions by solving Poisson's equation. This approximated approach has been implemented to simulate the dynamic admittance of nanoelectronic devices from first principles [7, 25].

2.2. Nonlinear-response current spectrum

2.2.1. General consideration and wide-band limit.
In the nonlinear-response regime, the first-order expansion, equation (2), as well as the resulting equations (4) and (5), become inadequate. In such a case, the complete knowledge on the two-time nonequilibrium Green's functions is required for calculating the transient current. However, the EOM of $G^{\text{r},<}(t, \tau)$ are coupled integro-differential equations, and thus extremely difficult to solve. To circumvent this problem, we resort to a formally exact formalism, developed in [7], for the transient electronic dynamics of open noninteracting systems. Its final form is an EOM for the RSDM $\sigma(t)$ of the reduced system as follows [7]:

$$\dot{\sigma}(t) = -\frac{\text{i}}{\hbar}[h(t), \sigma(t)] - \frac{1}{\hbar}\sum_\alpha Q_\alpha(t). \qquad (7)$$

Here, $Q_\alpha(t)$ characterizes the dissipative interaction between the system and lead α. The voltages are turned on from $t = 0$. The time-dependent current through the lead α is simply

$$I_\alpha(t) = -\frac{e}{\hbar}\,\text{tr}[Q_\alpha(t)]. \qquad (8)$$

Two approximate schemes have been proposed to calculate $Q_\alpha(t)$. One is a complete second-order quantum dissipation theory [26]. Another involves the WBL treatment for any connecting lead by assuming a structureless band of infinite width. To obtain an exact analytical nonlinear-response current, in the following we shall adopt the latter scheme.

In the WBL, $Q_\alpha(t)$ can be obtained as (cf [7] for the detailed derivation)

$$Q_\alpha(t) = \Lambda_\alpha\sigma(t) + \sigma(t)\Lambda_\alpha + [P_\alpha(t) + \text{h.c.}], \qquad (9)$$

with $\Lambda_\alpha \equiv \Gamma_\alpha/2$, and

$$P_\alpha(t) = -\frac{1}{\pi}\int_{-\infty}^{\infty} \text{d}\epsilon\, f_\alpha(\epsilon)\left\{ \text{i}U(t)\frac{\text{e}^{\text{i}\int_0^t \text{d}\tau\,[\Delta_\alpha(\tau)+\epsilon]/\hbar}}{\epsilon - h(0) + \text{i}\Lambda}\Lambda_\alpha \right.$$
$$\left. + \int_0^t \text{d}\tau\, \text{e}^{\text{i}\epsilon(t-\tau)/\hbar} K^+_\alpha(t) K^-_\alpha(\tau)\Lambda_\alpha \right\}, \qquad (10a)$$

where $\Lambda \equiv \sum_\alpha \Lambda_\alpha$ and

$$U(t) = \exp_+\left\{-\frac{\text{i}}{\hbar}\int_0^t \text{d}\tau\,[h(\tau) - \text{i}\Lambda]\right\}, \qquad (10b)$$

$$K^\pm_\alpha(t) = \exp_\pm\left\{\mp\frac{\text{i}}{\hbar}\int_0^t \text{d}\tau\,[h(\tau) - \text{i}\Lambda - \Delta_\alpha(\tau)]\right\}. \qquad (10c)$$

2.2.2. Nonlinear response in single-lead systems.
For a single-lead system, the subscript α can be dropped for clarity, and the displacement current is just $-I(t)$ due to conservation of total electrons. Denote $X(\omega) \equiv \tilde{\mathcal{F}}[\sigma(t)]$, where $\tilde{\mathcal{F}}$ is the half-Fourier transform defined as $\tilde{\mathcal{F}}[\chi(t)] \equiv \int_0^\infty \chi(t)\,\text{e}^{\text{i}\omega t}\text{d}t$ for any function $\chi(t)$. In the WBL, taking the $\tilde{\mathcal{F}}$ operation for both sides of equation (7) while presuming a time-independent Hamiltonian h, we have

$$-\hbar\,\sigma_0 - \text{i}\hbar\,\omega X(\omega) = -\text{i}[\tilde{h}X(\omega) - X(\omega)\tilde{h}^\dagger] - A(\omega), \quad (11)$$

where $\sigma_0 \equiv \sigma(t = 0)$, $\tilde{h} \equiv h - \text{i}\Lambda$ and $A(\omega) \equiv \tilde{\mathcal{F}}[P(t) + \text{h.c.}]$. For each ω, $X(\omega)$ can be obtained by solving the linear problem of equation (11) with $A(\omega)$ known from equation (10), and the current spectrum is evaluated via $I(\omega) = -e\,\text{tr}[\sigma_0 + \text{i}\omega X(\omega)]$. While in principle the initial time $t = 0$ can be taken to be any instant, in practice a convenient choice is when the composite device-lead(s) system is in its equilibrium/ground state in the absence of external voltages.

An alternative and often more convenient route is to analyze the induced RSDM, $Y(t) \equiv \sigma(t) - \sigma(t = 0)$. The EOM for $Y(t)$ in the WBL is

$$\dot{Y} = -\frac{\text{i}}{\hbar}(\tilde{h}Y - Y\tilde{h}^\dagger) - \frac{1}{\hbar}(\delta P + \text{h.c.}), \qquad (12)$$

where $\delta P(t) \equiv P(t) - P(t = 0)$. Taking the $\tilde{\mathcal{F}}$ operation for both sides of equation (12) while noting that $Y(\omega) \equiv \tilde{\mathcal{F}}[Y(t)] = \tilde{\mathcal{F}}[\dot{Y}(t)]/(-\text{i}\omega)$, we have

$$-\text{i}\hbar\,\omega Y(\omega) = -\text{i}[\tilde{h}Y(\omega) - Y(\omega)\tilde{h}^\dagger] - B(\omega), \qquad (13)$$

which parallels equation (11) with zero initial $Y(t = 0)$. Here, $B(\omega) \equiv \tilde{\mathcal{F}}[\delta P + \text{h.c.}]$ and $I(\omega) = -e\,\text{tr}[\text{i}\omega Y(\omega)]$,

The specific form of $A(\omega)$ or $B(\omega)$ depends on the time dependence rather than the amplitude of the applied voltages. Therefore, equations (11) and (13) can achieve both the linear- and nonlinear-response current spectra through a single-lead system, as we will elaborate further in section 4.
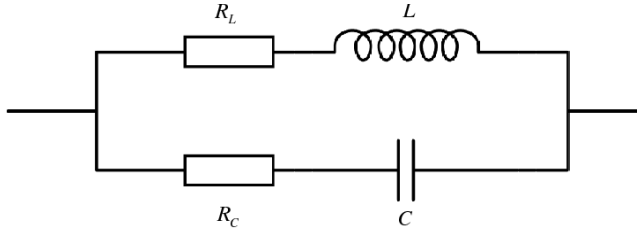
Figure 1. Equivalent classical circuit of a general two-terminal molecular device.

3. Linear-response dynamic admittance and equivalent circuit

Mapping quantum coherent transport properties of nanostructures to equivalent classical circuit representations has important implications in designing novel nanoelectronic devices. Recently, a classical circuit consisting of a resistor–capacitor (RC) branch and a resistor–inductor (RL) branch connected in parallel (see figure 1) has been proposed, which quantitatively characterizes the dynamical admittance of an aluminum–carbon nanotube–aluminum junction [25]. It has been expected that this RC–RL circuit can work for a general two-terminal molecular device. In this section, we will look into this issue by the derivation and analysis on the analytical admittance spectrum of model open systems.

Consider a system consisting of a single spinless level of energy ϵ_0, which is coupled to WBL leads with a total linewidth $\Gamma = \sum_\alpha \Gamma_\alpha$. Here, all the matrices of system dimension which appeared in section 2.1 reduce to scalars due to the only one system level in presence. Equation (6) thus reduces to

$$I_\alpha^{(1)}(\omega) = \frac{e}{h} \sum_\beta \frac{\Delta_\beta(\omega)}{\omega}\left(i\Gamma_\alpha\delta_{\alpha\beta} + \frac{\Gamma_\alpha\Gamma_\beta}{\hbar\omega + i\Gamma}\right)$$

$$\times \int d\epsilon\, [f(\epsilon) - f(\epsilon_+)][\bar{G}^r(\epsilon_+) - \bar{G}^a(\epsilon)]. \quad (14)$$

For a general two-lead conductor, the response current versus the applied external potential can be described by a 2×2 matrix with elements defined as

$$g_{\alpha\beta}(\omega) = I_\alpha(\omega)/V_\beta(\omega), \quad (15)$$

where $\alpha, \beta \in L, R$. The dynamic admittance is related to all the four response functions via

$$G(\omega) \equiv \tfrac{1}{4}[g_{LL}(\omega) + g_{RR}(\omega) - g_{LR}(\omega) - g_{RL}(\omega)]$$

$$= \frac{e^2}{h}\frac{i\hbar\omega\Gamma - 4\Gamma_L\Gamma_R}{4\omega(\hbar\omega + i\Gamma)}\int d\epsilon\, [f(\epsilon) - f(\epsilon_+)]$$

$$\times [\bar{G}^r(\epsilon_+) - \bar{G}^a(\epsilon)]. \quad (16)$$

We first adopt a symmetric coupling scheme with $\Gamma_L = \Gamma_R = \Gamma/2$. In this case, equation (16) reduces to

$$G(\omega) = \frac{e^2}{h}\frac{i\Gamma}{4\omega}\int d\epsilon\, [f(\epsilon) - f(\epsilon_+)][\bar{G}^r(\epsilon_+) - \bar{G}^a(\epsilon)]. \quad (17)$$

At zero temperature, the integral on the rhs of equation (17) can be evaluated analytically and then expanded in a Taylor series
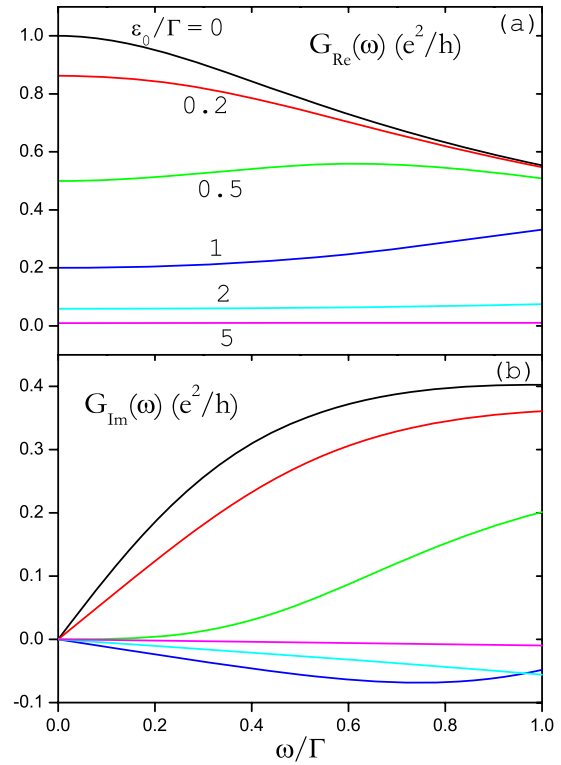

Figure 2. (a) The real and (b) imaginary parts of the dynamic admittance for a single-level system. The coupling to the two leads are symmetric, i.e. $\Gamma_L = \Gamma_R = \Gamma/2$. We present curves for the value of ϵ_0/Γ being 0, 0.2, 0.5, 1.0, 2.0 and 5.0, respectively.

of ω:

$$G(\omega) = \frac{e^2}{h}\frac{i\Gamma}{4\omega}\left\{\frac{1}{2}\ln\left[\frac{(\epsilon_0 + \hbar\omega)^2 + \Gamma^2/4}{\epsilon_0^2 + \Gamma^2/4}\right]\right.$$

$$+ \frac{1}{2}\ln\left[\frac{(\epsilon_0 - \hbar\omega)^2 + \Gamma^2/4}{\epsilon_0^2 + \Gamma^2/4}\right]$$

$$\left. + i\arctan\left(\frac{\epsilon_0 - \hbar\omega}{\Gamma/2}\right) - i\arctan\left(\frac{\epsilon_0 + \hbar\omega}{\Gamma/2}\right)\right\}$$

$$= \frac{e^2}{h}\left[\frac{\Gamma^2}{\Gamma^2 + 4\epsilon_0^2} + i\hbar\omega\frac{\Gamma(\Gamma^2 - 4\epsilon_0^2)}{(\Gamma^2 + 4\epsilon_0^2)^2}\right.$$

$$\left. + (\hbar\omega)^2\frac{4\Gamma^2(12\epsilon_0^2 - \Gamma^2)}{3(\Gamma^2 + 4\epsilon_0^2)^3} + \mathcal{O}(\omega^3)\right]. \quad (18)$$

It is clear that the dynamic admittance depends on the energy difference between the system level and the lead Fermi energy, $|\epsilon_0 - \mu_\alpha^{eq}| = |\epsilon_0|$. Hereafter, we will ignore the absolute value sign and use non-negative ϵ_0.

In figure 2, we plot the low-frequency dynamic admittance at various values of ϵ_0. Figure 2(a) depicts the conductance (real part of admittance) of the single-level system. As ϵ_0 increases, the conductance decreases to zero, indicating that the energy level far away from the chemical potential μ_α does not contribute to the conductance [2]. Figure 2(b) displays the susceptance (imaginary part of the admittance). It is apparent that, for $\epsilon_0 < \Gamma/2$, $G(\omega)$ is overall inductive (the leading term of its imaginary part is positive); while for $\epsilon_0 > \Gamma/2$, it is overall capacitive (the leading term of its imaginary part is negative) [12].
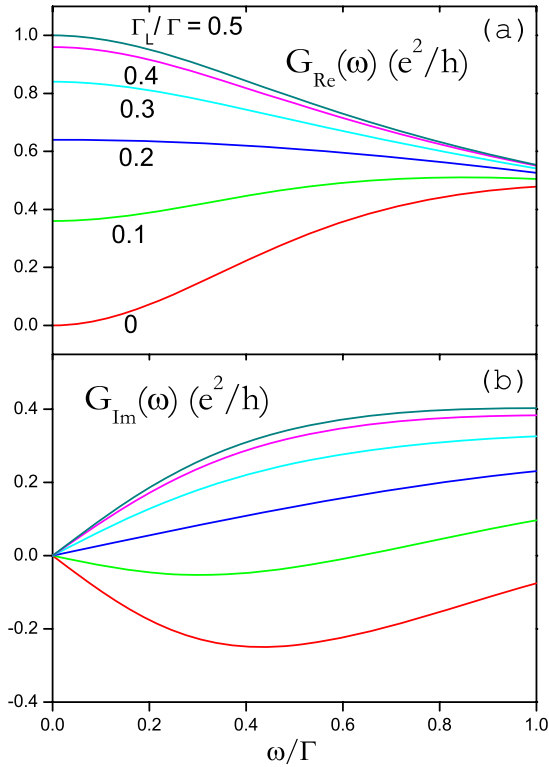
Figure 3. (a) The real and (b) imaginary parts of the dynamic admittance for a single-level system with system-level energy $\epsilon_0 = 0$. We present curves for the value of Γ_L / Γ being $0.5, 0.4, 0.3, 0.2, 0.1$ and 0, respectively.

Next, we exploit how the symmetry of system–lead couplings affects the dynamic admittance. The system-level energy ϵ_0 is set to be zero. Shown in figure 3 are (a) the real and (b) imaginary parts of dynamic admittance with Γ_L / Γ varying from 0.5 to 0, i.e. from the exactly symmetric coupling to extremely asymmetric coupling scenario. The dc conductance (the real part of admittance at $\omega = 0$) reaches its maximum value of e^2/h in the symmetric coupling limit. It reduces continuously as the couplings become more asymmetric, and vanishes in the limit of $\Gamma_L / \Gamma = 0$. We also note that, with the decrease of the ratio Γ_L / Γ, the overall effect of the susceptance varies from inductive to capacitive.

Now we try to map the quantum dynamic admittance of a two-lead conductor to an equivalent classical circuit. There are some basic requirements for the proposed circuit: (a) the dc current component should reproduce the Landauer–Büttiker steady-state current, (b) the ac behavior should be properly accounted for at the low-frequency regime and (c) in the extremely asymmetric coupling limit, such as $\Gamma_L \gg \Gamma_R \approx 0$, the classical circuit should correctly recover an RC circuit proposed earlier for a mesoscopic capacitor [8]. The simplest possible candidate which meets the above criteria is just the aforementioned RC–RL circuit as demonstrated in figure 1. Under ac bias voltages, its dynamic admittance, $G(\omega) = (R_C + \frac{1}{-i\omega C})^{-1} + (R_L - i\omega L)^{-1}$, assumes the following expansion form in the low-frequency range:

$$G(\omega) \simeq \frac{1}{R_L} - i\omega\left(C - \frac{L}{R_L^2}\right) + \omega^2\left(R_C C^2 - \frac{L^2}{R_L^3}\right). \quad (19)$$

The four elements, R_L and L of the RL branch, and R_C and C of the RC branch, are to be determined by the intrinsic system properties and some basic physical constants.

Consider the symmetric coupling cases, i.e. $\Gamma_L = \Gamma_R = \Gamma/2$. In steady states (only zero frequency is involved), the RC branch does not contribute to the dc current and L takes no effect, either. Therefore, the steady-state conductance uniquely determines the value of R_L to be

$$R_L = \frac{h}{e^2}\frac{\Gamma^2 + 4\epsilon_0^2}{\Gamma^2}. \quad (20)$$

The RC branch accounts for the charging effect associated with the coherent transport process. This can be confirmed as follows. Consider first a single-level system symmetrically coupled to two leads, i.e. $\Gamma_L = \Gamma_R = \Gamma/2$. The same time-dependent voltage is applied to both leads, i.e. $\Delta_L(t) = \Delta_R(t) = \Delta(t)$. The system-level shift, which can be controlled by a gate voltage or a substrate, is set to be zero. Due to the gauge invariance, this amounts to the system-level energy undergoing a time-dependent shift of $-\Delta(t)$ while the leads are voltage-free. The linear-response admittance, $G_\alpha(\omega) = \sum_\beta g_{\alpha\beta}(\omega)$ for arbitrary α, is obtained via equation (5) and then expanded in a Taylor series of ω up to the quadratic order as follows:

$$G(\omega) = \frac{e^2}{h}\left[-i\hbar\omega\frac{2\Gamma}{(\Gamma^2 + 4\epsilon_0^2)} + (\hbar\omega)^2\frac{4\Gamma^2}{(\Gamma^2 + 4\epsilon_0^2)^2} + \mathcal{O}(\omega^3)\right]. \quad (21)$$

This expansion can be readily fitted to the dynamic admittance of an RC branch so that the parameter of each circuit element is extracted. In doing so we arrive at

$$C = \frac{2e^2}{h}\frac{\Gamma}{\Gamma^2 + 4\epsilon_0^2} \quad \text{and} \quad R_C = \frac{h}{e^2}. \quad (22)$$

Similarly, we can extend the fitting to the single-level system that is coupled to n identical leads and obtained the R_C and C values as

$$C_n = \frac{1}{n}\left(\frac{e^2}{h}\frac{4\Gamma}{\Gamma^2 + 4\epsilon_0^2}\right) \quad \text{and} \quad R_n = \frac{nh}{2e^2}, \quad (23)$$

for the n-lead case. In particular, for $n = 1$, we have

$$C = \frac{e^2}{h}\frac{4\Gamma}{\Gamma^2 + 4\epsilon_0^2} \quad \text{and} \quad R_C = \frac{h}{2e^2}, \quad (24)$$

which recovers exactly Büttiker *et al*'s result [8]. Apparently, the charge relaxation resistance R_C is universal, regardless of the transmission detail; while C is dependent on ϵ_0. When the system is far away from resonance, i.e. $\epsilon_0 \gg \Gamma/2$, the capacitance goes to zero, indicating that the RC branch is nearly an open circuit. Hereafter, we assume that the system is near resonance, i.e. $\epsilon_0 < \Gamma/2$, without specification.

The obtained value of R_C, as well as the R_L already settled by equation (20), are then adopted for further determination of the L and C values. By comparing (18) and equation (19) up to second order in ω, we have

$$L = \frac{h}{e^2}\frac{7}{6\Gamma}\left[1 - \frac{19}{12}\left(\frac{2\epsilon_0}{\Gamma}\right)^2\right],$$

$$C = \frac{e^2}{h}\frac{1}{6\Gamma}\left[1 - \frac{85}{12}\left(\frac{2\epsilon_0}{\Gamma}\right)^2\right]. \quad (25)$$

4. Response current through a single-lead system under applied voltages of different time dependence

Under a large external voltage, the electronic dynamics of the reduced system goes beyond the linear-response regime. In such a case, the dynamic admittance involves higher-frequency components, and equivalent classical circuits are no longer adequate for even a qualitative description of the electronic response. The nonlinear-response current depends explicitly on the time dependence of the applied voltage, and hence needs to be studied case by case. In this section, we present an analytical response current spectrum for a single-lead system, $I(\omega) = \mathcal{F}[I(t)] = \tilde{\mathcal{F}}[I(t)]$ (the last equality is due to the fact that $I(t) = 0$ at $t < 0$), under step, delta and sinusoidal voltages. Since $I(t)$ is real in time, we immediately have the following symmetries for the response current spectrum: $\mathrm{Re}[I(\omega)] = \mathrm{Re}[I(-\omega)]$ and $\mathrm{Im}[I(\omega)] = -\mathrm{Im}[I(-\omega)]$.

4.1. Response current spectrum under a step-function voltage

Consider a step-function voltage switched on at time $t = 0$, i.e. $\Delta(t) \equiv -eV(t) = \Delta\Theta(t)$, where $\Theta(t)$ is the Heaviside step function and Δ the voltage amplitude. Since the magnitude of Δ is not confined, we can go beyond the linear-response regime by adopting an arbitrarily large Δ. Under a step voltage, the time derivative of $\delta P(t)$ introduced after equation (12) is

$$\delta\dot{P} = \frac{2\Delta}{\pi}\int_{-\infty}^{+\infty}\mathrm{d}\epsilon\, f(\epsilon)\frac{\mathrm{e}^{\mathrm{i}(\epsilon+\Delta-\tilde{h})t/\hbar}}{\epsilon-\tilde{h}}\Lambda. \tag{26}$$

Denote $C(\omega) \equiv \tilde{\mathcal{F}}[\delta\dot{P} + \text{h.c.}]$, and hence by definition $B(\omega) = C(\omega)/(-\mathrm{i}\omega)$; cf equation (13). At a finite temperature $T > 0$, $C(\omega)$ is expressed as follows (setting the Boltzmann constant $k_B = 1$ hereafter):

$$C(\omega) = 2\Delta T\sum_{m=0}^{\infty}[(\hbar\omega + \Delta + \gamma_m - \tilde{h})^{-1}(\gamma_m - \tilde{h})^{-1}\Lambda$$
$$+ \Lambda(\hbar\omega - \Delta + \gamma_m + \tilde{h}^{\dagger})^{-1}(\gamma_m + \tilde{h}^{\dagger})^{-1}] \tag{27}$$

with $\gamma_m = \mathrm{i}(2m+1)\pi T$. $I(\omega)$ is then obtained via solving the linear equation (13).

In particular, for a system of a single spinless level of energy ϵ_0, all the matrices of system dimension reduce to scalars. For such a simple system, numerically exact time-dependent current has been reported based on the NEGF approach [27, 28]. The (same) exact $I(t)$ can be achieved alternatively via an inverse Fourier transform of $I(\omega)$ as given below. At $T = 0$

$$I(\omega) = \frac{-e\Gamma\Delta}{2\pi(\hbar\omega + \mathrm{i}\Gamma)}\left\{\frac{1}{\hbar\omega + \Delta}\right.$$
$$\times\left\{\frac{1}{2}\ln\left[\frac{(\hbar\omega + \hbar\omega_0)^2 + (\Gamma/2)^2}{\epsilon_0^2 + (\Gamma/2)^2}\right]\right.$$
$$\left.-\mathrm{i}\left[\arctan\left(\frac{\hbar\omega + \hbar\omega_0}{\Gamma/2}\right) + \arctan\left(\frac{\epsilon_0}{\Gamma/2}\right)\right]\right\}$$
$$+ \frac{1}{\hbar\omega - \Delta}\left\{\frac{1}{2}\ln\left[\frac{(\hbar\omega - \hbar\omega_0)^2 + (\Gamma/2)^2}{\epsilon_0^2 + (\Gamma/2)^2}\right]\right.$$
$$\left.\left.-\mathrm{i}\left[\arctan\left(\frac{\hbar\omega - \hbar\omega_0}{\Gamma/2}\right) - \arctan\left(\frac{\epsilon_0}{\Gamma/2}\right)\right]\right\}\right\}. \tag{28}$$

While at $T > 0$, we have

$$I(\omega) = \frac{\mathrm{i}e\Gamma\Delta T}{\hbar\omega + \mathrm{i}\Gamma}\sum_{m=0}^{\infty}\{(\epsilon_0 - \mathrm{i}\Gamma_m)^{-1}[(\hbar\omega + \hbar\omega_0) + \mathrm{i}\Gamma_m]^{-1}$$
$$- (\epsilon_0 + \mathrm{i}\Gamma_m)^{-1}[(\hbar\omega - \hbar\omega_0) + \mathrm{i}\Gamma_m]^{-1}\}$$
$$= \frac{e\Delta\Gamma}{\hbar\omega + \mathrm{i}\Gamma}\left\{\frac{1}{\hbar\omega + \Delta}\left[\phi\left(\frac{1}{2} + \frac{\Gamma/2 + \mathrm{i}\epsilon_0}{2\pi T}\right)\right.\right.$$
$$\left.- \phi\left(\frac{1}{2} + \frac{\Gamma/2 - \mathrm{i}\hbar\omega - \mathrm{i}\hbar\omega_0}{2\pi T}\right)\right] + \frac{1}{\Delta - \hbar\omega}$$
$$\times\left[\phi\left(\frac{1}{2} + \frac{\Gamma/2 + \mathrm{i}\hbar\omega_0 - \mathrm{i}\hbar\omega}{2\pi T}\right)\right.$$
$$\left.\left.- \phi\left(\frac{1}{2} + \frac{\Gamma/2 - \mathrm{i}\epsilon_0}{2\pi T}\right)\right]\right\}. \tag{29}$$

Here $\hbar\omega_0 \equiv \Delta - \epsilon_0$, $\Gamma_m \equiv \Gamma/2 - \mathrm{i}\gamma_m$ and $\phi(x)$ is a digamma function of x.

When the step amplitude Δ is sufficiently small, $I(\omega)$ obtained via equations (28) and (29) should recover the correct linear-response admittance $G(\omega)$, which had been studied extensively [8–11] and was already attained in section 3 on a two-lead system in the extremely asymmetric coupling limit. In this case, it is well known that the quantum coherent dynamics can be mapped to an RC circuit with its complex impedance (the reciprocal of admittance) as follows:

$$[G(\omega)]^{-1} = R_q + \frac{1}{-\mathrm{i}\omega C}. \tag{30}$$

An important property of equation (30) is that R_q should be an ω-independent constant except at the removable singularity $\omega = 0$. It was predicted that, at $T = 0$, the real impedance amounts exactly to half a resistance quantum, i.e. $R_q = h/(2e^2)$ [8, 11]. Indeed, it can be shown that, based on equation (28), we have (see appendix B for details)

$$R_q = \lim_{\Delta\to 0}\lim_{\omega\to 0^+}\lim_{\delta\to 0^+}\mathrm{Re}\left[-\frac{\Delta^\delta(\omega)}{I(\omega)}\right] = \frac{h}{2e^2} \tag{31}$$

at $T = 0$ and $\epsilon_0 = 0$, where

$$\Delta^\delta(\omega) \equiv \mathcal{F}[\Delta(t)\mathrm{e}^{-\delta t}] = \frac{\mathrm{i}\Delta}{\omega + \mathrm{i}\delta}. \tag{32}$$

The three limit operations in equation (31) *cannot* be interchanged.

It is important to note that the system-level energy is distinctly resolved in the response current spectrum. In figure 4 we plot $I(\omega)$ under step voltages of various amplitudes. It is interesting to see the real (imaginary) part of $I(\omega)$ exhibits a peak/dip (wiggle) centered precisely at $\hbar\omega = |\Delta - \epsilon_0|$. This characteristic resonance feature of $I(\omega)$ can be identified easily from both equation (28) and the rhs of the first equality of equation (29). This resonance signature stands in both linear- and nonlinear-response regimes, and can be trivially extended to an open system of a number of uncorrelated levels. Therefore, it may be employed to determine the intrinsic level energies of a few-electron quantum dot via the experimentally measured transient response current to manually controlled step voltage pulses.
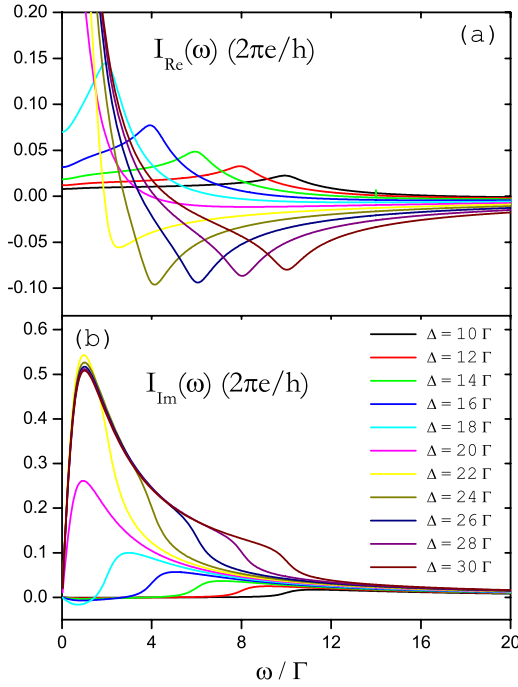
Figure 4. (a) Real and (b) imaginary parts of $I(\omega)$ for a single-level system under a step voltage pulse. The lines represent different voltage amplitudes. The other parameters adopted are: $T = 0$ and $\epsilon_0 = 20\Gamma$.

4.2. Response current spectrum under a delta-function voltage

For a delta-function voltage, i.e. $\Delta(t) = \Delta\Theta(t)\delta(t)$ and δP is expressed as

$$\delta P = \frac{\mathrm{i}}{\pi}[1 - \mathrm{e}^{\mathrm{i}\Delta/(2\hbar)}]\int_{-\infty}^{+\infty} \mathrm{d}\epsilon\, f(\epsilon)\frac{\mathrm{e}^{\mathrm{i}(\epsilon - \tilde{h})t/\hbar}}{\epsilon - \tilde{h}}\Lambda. \tag{33}$$

At $T > 0$, $B(\omega)$ involved in equation (13) assumes the following form:

$$B(\omega) = \mathrm{i}(2T)\sum_{m=0}^{\infty}\left[\frac{1 - \mathrm{e}^{\mathrm{i}\Delta/(2\hbar)}}{(\hbar\omega + \gamma_m - \tilde{h})(\gamma_m - \tilde{h})}\Lambda\right.$$
$$\left. - \Lambda\frac{1 - \mathrm{e}^{-\mathrm{i}\Delta/(2\hbar)}}{(\hbar\omega + \gamma_m + \tilde{h}^\dagger)(\gamma_m + \tilde{h}^\dagger)}\right]. \tag{34}$$

$I(\omega)$ can then be evaluated via solving the linear equation (13).

In particular, for a system consisting of a single spinless level of energy ϵ_0, we finally have

$$I(\omega) = -\frac{e\Gamma}{2\pi(\hbar\omega + \mathrm{i}\Gamma)}\left\{\frac{\mathrm{e}^{\mathrm{i}\Delta/(2\hbar)} - 1}{2}\right.$$
$$\times\left\{\ln\left[\frac{\epsilon_0^2 + (\Gamma/2)^2}{(\epsilon_0^-)^2 + (\Gamma/2)^2}\right]\right.$$
$$\left. + 2\mathrm{i}\left[\arctan\left(\frac{\epsilon_0}{\Gamma/2}\right) - \arctan\left(\frac{\epsilon_0^-}{\Gamma/2}\right)\right]\right\}$$
$$+ \frac{1 - \mathrm{e}^{-\mathrm{i}\Delta/(2\hbar)}}{2}\left\{\ln\left[\frac{\epsilon_0^2 + (\Gamma/2)^2}{(\epsilon_0^+)^2 + (\Gamma/2)^2}\right]\right.$$
$$\left.\left. - 2\mathrm{i}\left[\arctan\left(\frac{\epsilon_0}{\Gamma/2}\right) - \arctan\left(\frac{\epsilon_0^+}{\Gamma/2}\right)\right]\right\}\right\} \tag{35}$$

at $T = 0$ with $\epsilon_0^\pm = \epsilon_0 \pm \hbar\omega$. At $T > 0$, we arrive at

$$I(\omega) = \frac{\mathrm{i}e\hbar\omega\Gamma T}{\hbar\omega + \mathrm{i}\Gamma}\sum_{m=0}^{\infty}\left[\frac{\mathrm{e}^{\mathrm{i}\Delta/(2\hbar)} - 1}{(\epsilon_0^- - \mathrm{i}\Gamma_m)(\epsilon_0 - \mathrm{i}\Gamma_m)}\right.$$
$$\left. + \frac{1 - \mathrm{e}^{-\mathrm{i}\Delta/(2\hbar)}}{(\epsilon_0^+ + \mathrm{i}\Gamma_m)(\epsilon_0 + \mathrm{i}\Gamma_m)}\right]$$
$$= \frac{-e\Gamma}{\pi(\hbar\omega + \mathrm{i}\Gamma)}\left\{\left[\phi\left(\frac{1}{2} + \frac{\Gamma/2 + \mathrm{i}\epsilon_0^-}{2\pi T}\right)\right.\right.$$
$$\left. - \phi\left(\frac{1}{2} + \frac{\Gamma/2 + \mathrm{i}\epsilon_0}{2\pi T}\right)\right][1 - \mathrm{e}^{\mathrm{i}\Delta/(2\hbar)}]$$
$$- [1 - \mathrm{e}^{-\mathrm{i}\Delta/(2\hbar)}]\left[\phi\left(\frac{1}{2} + \frac{\Gamma/2 - \mathrm{i}\epsilon_0^+}{2\pi T}\right)\right.$$
$$\left.\left. - \phi\left(\frac{1}{2} + \frac{\Gamma/2 - \mathrm{i}\epsilon_0}{2\pi T}\right)\right]\right\}. \tag{36}$$

It is readily verified that the current spectrum can be factorized as $I(\omega) = \sin(\frac{\Delta}{2\hbar})K(\omega)$ at resonance ($\epsilon_0 = \mu^{\mathrm{eq}} = 0$), where $K(\omega)$ is a certain complex function independent of Δ.

The linear-response admittance, $G(\omega) = I(\omega)/V(\omega)$, does not rely on the specific time-dependent form of the applied voltage. However, the delta-function form is most convenient in achieving $G(\omega)$, both analytically and numerically. This is due to the fact that $V(\omega) = -\Delta(\omega)/e = -\Delta/(2e)$ is an ω-independent constant. In this sense, we have $I(\omega) \propto G(\omega)$ for any Δ. In particular, for a sufficiently small Δ, $\mathrm{e}^{\mathrm{i}\Delta/(2\hbar)} - 1 \approx 1 - \mathrm{e}^{-\mathrm{i}\Delta/(2\hbar)} \approx \mathrm{i}\Delta/(2\hbar)$, and equation (35) leads to

$$G(\omega) = \frac{e^2}{\hbar}\frac{\mathrm{i}\Gamma}{2\pi(\hbar\omega + \mathrm{i}\Gamma)}\left\{\frac{1}{2}\ln\{[\epsilon_0^2 + (\Gamma/2)^2]^2\right.$$
$$\times [(\epsilon_0^-)^2 + (\Gamma/2)^2]^{-1}[(\epsilon_0^+)^2 + (\Gamma/2)^2]^{-1}\}$$
$$\left. + \mathrm{i}\left[\arctan\left(\frac{\epsilon_0^+}{\Gamma/2}\right) - \arctan\left(\frac{\epsilon_0^-}{\Gamma/2}\right)\right]\right\}, \tag{37}$$

which recovers equation (3) in [10].

Similar to the step voltage case, the relative position of the system level with respect to μ^{eq} is reflected in $I(\omega)$ under a delta voltage pulse. Figure 5 depicts $I(\omega)$ at $T = 0$ for various ϵ_0 ranging from negative (lower than μ^{eq}) to positive (higher than μ^{eq}) values. Different from that in figure 4, now the resonance signature appears at the frequency $\hbar\omega = |\epsilon_0|$, independent of the value of Δ.

4.3. Response current spectrum under a sinusoidal voltage

Now we turn to a cosine-function voltage, $\Delta(t) = \Delta\Theta(t)\cos(\Omega t)$, with Ω being the driving frequency. To get away from the tricky divergence, we start from the EOM for $\sigma(t)$ (equation (7)) instead of that for the induced RSDM (equation (12)). Note that $\mathrm{e}^{\frac{\mathrm{i}}{\hbar}\int_0^t \Delta(\tau)\mathrm{d}\tau} = \mathrm{e}^{\mathrm{i}(\frac{\Delta}{\hbar\Omega})\sin(\Omega t)} = \sum_{k=-\infty}^{\infty} J_k(\frac{\Delta}{\hbar\Omega})\mathrm{e}^{\mathrm{i}k\Omega t}$, where $J_k(x)$ is the kth Bessel function of the first kind. Without loss of generality, we consider the
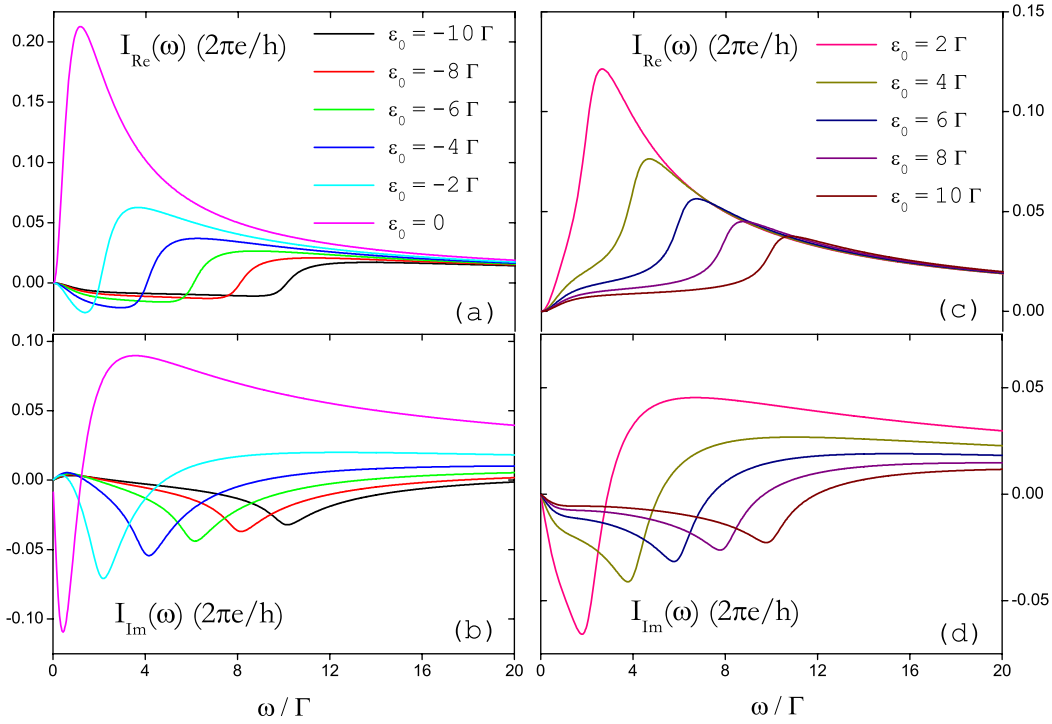
Figure 5. (a) and (c) Real and (b) and (d) imaginary parts of $I(\omega)$ for a single-level system under a delta voltage pulse. The lines represent different ϵ_0. The other parameters adopted are: $T = 0$ and $\Delta = 20\Gamma$.

case of $\frac{\Delta}{\hbar\Omega} > 0$. After some straightforward algebra, we have

$$\tilde{\mathcal{F}}[\boldsymbol{P}^+ + \text{h.c.}] = \frac{1}{\pi} \sum_{k,p=-\infty}^{\infty} (-1)^k \frac{J_k(\frac{\Delta}{\hbar\Omega}) J_p(\frac{\Delta}{\hbar\Omega})}{\omega + (k+p)\Omega}$$

$$\times \int_{-\infty}^{\infty} d\epsilon\, f(\epsilon) \left[\frac{1}{\epsilon_+ + p\hbar\Omega - \tilde{\boldsymbol{h}}} \boldsymbol{\Lambda} \right.$$

$$\left. - \boldsymbol{\Lambda} \frac{1}{\epsilon_- - k\hbar\Omega - \tilde{\boldsymbol{h}}^\dagger} \right], \tag{38}$$

$$\tilde{\mathcal{F}}[\boldsymbol{P}^- + \text{h.c.}] = -\frac{1}{\pi} \sum_{k=-\infty}^{\infty} J_k\left(\frac{\Delta}{\hbar\Omega}\right) \int_{-\infty}^{\infty} d\epsilon\, f(\epsilon)$$

$$\times \left\{ \left[\frac{1}{\epsilon_+ + k\hbar\Omega - \tilde{\boldsymbol{h}}} - \frac{1}{\epsilon - \tilde{\boldsymbol{h}}} \right] \frac{\boldsymbol{\Lambda}}{\omega + k\Omega} - \frac{\boldsymbol{\Lambda}}{\omega - k\Omega} \right.$$

$$\times \left. \left[\frac{1}{\epsilon_- + k\hbar\Omega - \tilde{\boldsymbol{h}}^\dagger} - \frac{1}{\epsilon - \tilde{\boldsymbol{h}}^\dagger} \right] \right\}. \tag{39}$$

Therefore, $A(\omega)$ required for equation (11) is obtained by combining the rhs of equations (38) and (39). $I(\omega)$ is then readily evaluated after solving the linear problem equation (11).

In particular, for a system consisting of a single spinless level of energy ϵ_0, the solution of equation (11) leads to

$$I(\omega) = -e \frac{\mathrm{i}\Gamma\sigma_0 + \omega A(\omega)}{\hbar\omega + \mathrm{i}\Gamma}, \tag{40}$$

where $\sigma_0 = 1/2 - \arctan(2\epsilon_0/\Gamma)/\pi$ at $T = 0$, and $A(\omega)$ is simply the sum of the rhs of equations (38) and (39), with all involving matrices of system dimension reduce to scalars. At any temperature T, the integrations over ϵ involved in equations (38) and (39) can be done analytically as in

sections 4.1 and 4.2. The tedious complete expression of $A(\omega)$ is left to appendix C. Here, we demonstrate both the linear- and nonlinear-response current spectra in figure 6. It is apparent from figure 6 and from the poles in equations (38) and (39) that the resonance signals arise at the exact multiples of the driving frequency Ω. In the linear-response regime, the current appears almost exclusively at the 'fundamental frequency' Ω with overall small magnitude; see figure 6(a). As the voltage amplitude is enlarged, the overtone components gain more importance. For instance, with the Δ as large as 5Γ, up to the second overtone (corresponding to $\omega = 3\Omega$) can be observed distinctly in $I(\omega)$; see figure 6(b).

5. Concluding remarks

The linear-response quantum coherent dynamics of a general two-terminal conductor is well characterized by an equivalent classical RL–RC circuit, which expresses the dynamic admittance accurate up to the quadratic order in frequency. For systems comprised of a single level, the electronic admittance ranges from an overall inductive behavior in the near-to-resonance cases to a capacitive-insulating feature in far-from-resonance cases. As the coupling strength between the system level and one of the leads weakens continuously, the RL branch becomes trivial and the RC branch recovers gradually the values for a single-lead capacitor.

The nonlinear-response current spectrum are conspicuously different under various types of applied voltages. For a single-lead system, transient response current often exhibits rapid oscillations on top of an exponential decay [15]. The exponential profile corresponds to the factor $(\hbar\omega + \mathrm{i}\Gamma)^{-1}$ in
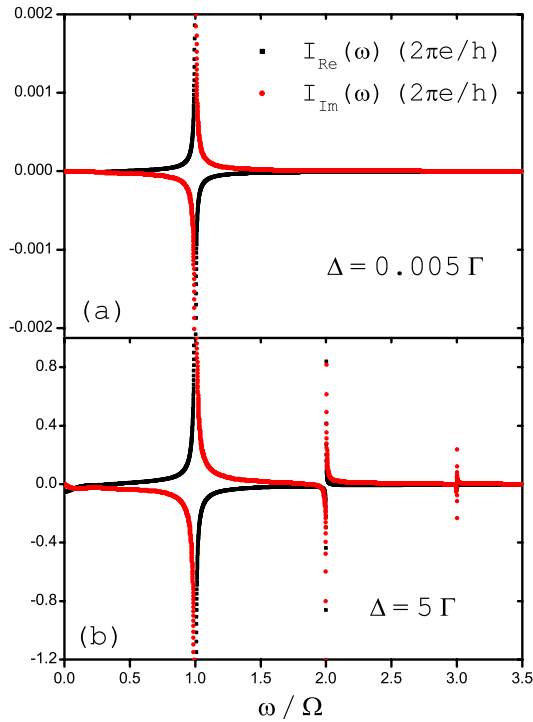
Figure 6. Real and imaginary parts of current spectrum for a single-level system driven by a cosine-function voltage with the amplitude of (a) $\Delta = 0.005\Gamma$ and (b) $\Delta = 5\Gamma$. Other parameters adopted are $T = 0$, $\epsilon_0 = -2.5\Gamma$ and $\Omega = 10\Gamma$.

$I(\omega)$, which is manifested in the low-frequency range; see, for instance, equations (28) and (35). The rapid oscillations of the time-dependent current originate from the rest of the parts of $I(\omega)$, which reflect either the energetic configuration of the reduced system or the characteristics of the driving voltage, depending on the case. For systems consisting of a single level, the level energy ϵ_0 is resolved distinctly at the frequency $\hbar\omega = |\Delta - \epsilon_0|$ and $\hbar\omega = |\epsilon_0|$ under step- and delta-function voltages, respectively. However, ϵ_0 is not explicitly expressed by a sinusoidal voltage. Instead, the driving voltage frequency is clearly manifested in the response current spectrum.

For a realistic molecular device, first-principles simulations have been carried out to mimic its current response to time-dependent voltages applied to the leads [7]. The calculations are based on a time-dependent density-functional theory (TDDFT) [29] for open systems. Within the framework of TDDFT, an effective noninteracting system, the Kohn–Sham reference system [30], is treated explicitly. The transient current in response to an applied voltage is obtained by solving the time evolution of the Kohn–Sham system [22]. In principle this approach would yield the exact dynamics of any realistic system, provided that the exact exchange-correlation functional and dissipation functional were known. Therefore, combining first-principles simulations and analytical results of admittance and current spectra presents a new direction in design and implementation of nanoelectronic devices.

Acknowledgments

Appendix A. Derivation of linear-response current

Consider a noninteracting open system which is characterized by the single-electron Hamiltonian $h(t)$. Its linear-response transient current under an applied voltage is expressed as equation (2). To evaluate the response current spectrum $I_\alpha(\omega) \equiv \mathcal{F}[I_\alpha(t)]$, we need to know the first-order changes of G^{r}, $G^{<}$, $\Sigma^{\mathrm{r,a}}$ and $\Sigma^{<}$. The first-order changes of the self-energies can be evaluated with equation (3), while the first-order changes of the Green's functions can be evaluated by solving the following Dyson's equations:

$$G^{\mathrm{r}}(t, \tau) = g^{\mathrm{r}}(t, \tau) + \int \mathrm{d}\tau_1 \int \mathrm{d}\tau_2 \, g^{\mathrm{r}}(t, \tau_1)\Sigma^{\mathrm{r}}(\tau_1, \tau_2)$$
$$\times G^{\mathrm{r}}(\tau_2, \tau), \tag{A.1a}$$
$$G^{<}(t, \tau) = \int \mathrm{d}t_1 \int \mathrm{d}t_2 \, G^{\mathrm{r}}(t, t_1)\Sigma^{<}(t_1, t_2)G^{\mathrm{a}}(t_2, \tau), \tag{A.1b}$$

where $g^{\mathrm{r}}(t, \tau)$ is the retarded Green's function of the isolated system.

For a time-independent system Hamiltonian, i.e. $h(t) = h$, $\delta G^{\mathrm{r}}(t, \tau)$ originates solely from the first-order change of the retarded self-energy as follows:

$$\delta G^{\mathrm{r}}(t, \tau) = \int \mathrm{d}\tau_1 \int \mathrm{d}\tau_2 \, \bar{g}^{\mathrm{r}}(t - \tau_1) \, \delta\Sigma^{\mathrm{r}}(\tau_1, \tau_2)$$
$$\times \bar{G}^{\mathrm{r}}(\tau_2 - \tau) + \int \mathrm{d}\tau_1 \int \mathrm{d}\tau_2 \, \bar{g}^{\mathrm{r}}(t - \tau_1)$$
$$\times \bar{\Sigma}^{\mathrm{r}}(\tau_1 - \tau_2) \, \delta G^{\mathrm{r}}(\tau_2, \tau). \tag{A.2}$$

Equation (A.2) is actually a recursive relation for $\delta G^{\mathrm{r}}(t, \tau)$, so that its rhs can be expanded further to an infinite series, and each term in the series would contain $\delta\Sigma^{\mathrm{r}}$ as part of the integrand. The first-order change of the lesser Green's function is

$$\delta G^{<}(t, \tau) = \int \mathrm{d}t_1 \int \mathrm{d}t_2 \, [\delta G^{\mathrm{r}}(t, t_1)\bar{\Sigma}^{<}(t_1 - t_2)$$
$$\times \bar{G}^{\mathrm{a}}(t_2 - \tau) + \bar{G}^{\mathrm{r}}(t - t_1)\delta\Sigma^{<}(t_1, t_2)$$
$$\times \bar{G}^{\mathrm{a}}(t_2 - \tau) + \bar{G}^{\mathrm{r}}(t - t_1)\bar{\Sigma}^{<}(t_1 - t_2)$$
$$\times \delta G^{\mathrm{a}}(t_2, \tau)]. \tag{A.3}$$

By inserting equations (3), (A.2) and (A.3) into equation (2) and taking a double Fourier transform, the final expression of response current spectrum $I_\alpha^{(1)}(\omega)$, equations (4) and (5), is achieved.

If a time-dependent system Hamiltonian is considered, i.e. $h(t) = h + \Delta_{\mathrm{D}}(t)$, an additional term would arise on the rhs of equation (5), which originates from the deviation of $g^{\mathrm{r}}(t, \tau)$ from its equilibrium counterpart $\bar{g}^{\mathrm{r}}(t - \tau)$:

$$\delta g^{\mathrm{r}}(t, \tau) \equiv g^{\mathrm{r}}(t, \tau) - \bar{g}^{\mathrm{r}}(t - \tau)$$
$$= \frac{1}{2\pi} \int \frac{\mathrm{d}\omega}{\omega} \, \Delta_{\mathrm{D}}(\omega)(\mathrm{e}^{-\mathrm{i}\omega t} - \mathrm{e}^{-\mathrm{i}\omega\tau})\bar{g}^{\mathrm{r}}(t - \tau), \tag{A.4}$$

where $\Delta_{\mathrm{D}}(\omega) \equiv \mathcal{F}[\Delta_{\mathrm{D}}(t)]$. The additional contribution to the response current spectrum is

$$I_\alpha'(\omega) = \frac{e}{h}\frac{\Delta_{\mathrm{D}}(\omega)}{\omega} \int \mathrm{d}\epsilon \, \mathrm{tr}[\mathcal{G}_{\alpha\beta}'(\epsilon; \omega)], \tag{A.5}$$

with

$$\mathcal{G}'_{\alpha\beta} = \check{\Sigma}^{\mathrm{r}}_{\alpha}\bar{G}^{<} + \check{\Sigma}^{<}_{\alpha}\bar{G}^{\mathrm{a}} - \bar{G}^{<}_{+}\check{\Sigma}^{\mathrm{a}}_{\alpha} - \bar{G}^{\mathrm{r}}_{+}\check{\Sigma}^{<}_{\alpha}$$
$$- \bar{G}^{\mathrm{r}}_{+}\check{\Sigma}^{\mathrm{r}}(\bar{G}^{<}\bar{\Sigma}^{\mathrm{a}}_{\alpha} + \bar{G}^{\mathrm{r}}\bar{\Sigma}^{<}_{\alpha}) - (\bar{G}^{<}_{+}\check{\Sigma}^{\mathrm{a}} + \bar{G}^{\mathrm{r}}_{+}\check{\Sigma}^{<})$$
$$\times \bar{G}^{\mathrm{a}}\bar{\Sigma}^{\mathrm{a}}_{\alpha} + (\bar{\Sigma}^{\mathrm{r}}_{\alpha}\bar{G}^{<} + \bar{\Sigma}^{<}_{\alpha}\bar{G}^{\mathrm{a}})_{+}\check{\Sigma}^{\mathrm{a}}\bar{G}^{\mathrm{a}}$$
$$+ (\bar{\Sigma}^{\mathrm{r}}_{\alpha}\bar{G}^{\mathrm{r}})_{+}(\check{\Sigma}^{\mathrm{r}}\bar{G}^{<} + \check{\Sigma}^{<}\bar{G}^{\mathrm{a}}). \tag{A.6}$$

The total linear-response current is thus the combination of equations (4) and (A.5).

Appendix B. Charge relaxation resistance under a step voltage

Consider the resonance case of $\epsilon_0 = \mu^{\mathrm{eq}} = 0$ at $T = 0$, with a slowly decaying exponential function attached to the step voltage pulse, i.e. $\Delta^{\delta}(t) = \Delta\Theta(t)\,\mathrm{e}^{-\delta t}$. From equation (28), the response current spectrum is

$$I(\omega) = -\frac{e\Delta\Lambda}{\pi(\hbar\omega + \mathrm{i}\Gamma)}[A_r(\omega) + \mathrm{i}A_i(\omega)], \tag{B.1}$$

with $A_r(\omega)$ and $A_i(\omega)$ being two real functions:

$$A_r(\omega) = \frac{1}{2}\left\{\frac{1}{\hbar\omega + \Delta}\ln\left[\frac{(\hbar\omega + \Delta)^2 + (\Gamma/2)^2}{\Gamma^2/4}\right]\right.$$
$$\left. + \frac{1}{\hbar\omega - \Delta}\ln\left[\frac{(\hbar\omega - \Delta)^2 + (\Gamma/2)^2}{\Gamma^2/4}\right]\right\}, \tag{B.2}$$

$$A_i(\omega) = -\frac{1}{\hbar\omega + \Delta}\arctan\left(\frac{\hbar\omega + \Delta}{\Gamma/2}\right)$$
$$- \frac{1}{\hbar\omega - \Delta}\arctan\left(\frac{\hbar\omega - \Delta}{\Gamma/2}\right). \tag{B.3}$$

Therefore, we have

$$\lim_{\delta\to 0^+}\mathrm{Re}\left[\frac{\Delta^{\delta}(\omega)}{I(\omega)}\right] = \left(\frac{2\pi}{e^2\Gamma}\right)$$
$$\times \mathrm{Im}\left[\frac{(\hbar\omega + \mathrm{i}\Gamma)(\omega - \mathrm{i}\delta)}{(\omega^2 + \delta^2)(A_r^2 + A_i^2)}(A_r - \mathrm{i}A_i)\right]\bigg|_{\delta\to 0^+}$$
$$= \left(\frac{h}{e^2\Gamma}\right)\left[\frac{\Gamma A_r - \omega A_i}{\omega(A_r^2 + A_i^2)}\right]. \tag{B.4}$$

Note that

$$\lim_{\Delta\to 0}\lim_{\omega\to 0^+}\left[\frac{A_r(\omega)}{\hbar\omega}\right] = \lim_{\Delta\to 0}\left[-\frac{1}{\Delta^2}\ln\left(1 + \frac{4\Delta^2}{\Gamma^2}\right)\right.$$
$$\left. + \frac{2}{\Delta^2 + \Gamma^2/4}\right] = \frac{4}{\Gamma^2}, \tag{B.5}$$

$$\lim_{\Delta\to 0}\lim_{\omega\to 0^+}A_i(\omega) = \lim_{\Delta\to 0}\left[-\frac{2}{\Delta}\arctan\left(\frac{2\Delta}{\Gamma}\right)\right] = -\frac{4}{\Gamma}. \tag{B.6}$$

Combining equations (B.4)–(B.6) finally leads to the expected linear-response R_q given by equation (31).

Appendix C. Analytical expression for $A(\omega)$ under a cosine-function voltage

The last piece of knowledge to achieve an analytical current spectrum $I(\omega)$ under a cosine voltage is the expression of $A(\omega)$. The integrations over ϵ involved in equations (38)

and (39) can be performed analytically by the residue theorem. We thus have

$$A(\omega) = \frac{\Lambda}{\pi}\sum_{k=-\infty}^{\infty}J_k\left(\frac{\Delta}{\hbar\Omega}\right)\left\{\frac{1}{\omega - k\Omega}\right.$$
$$\times\left\{\frac{1}{2}\ln\left[\frac{(\epsilon_0^+ - k\hbar\Omega)^2 + \Lambda^2}{\epsilon_0^2 + \Lambda^2}\right]\right.$$
$$\left. - \mathrm{i}\left[\arctan\left(\frac{\epsilon_0^+ - k\hbar\Omega}{\Lambda}\right) - \arctan\left(\frac{\epsilon_0}{\Lambda}\right)\right]\right\}$$
$$- \frac{1}{\omega + k\Omega}\left\{\frac{1}{2}\ln\left[\frac{(\epsilon_0^- - k\hbar\Omega)^2 + \Lambda^2}{\epsilon_0^2 + \Lambda^2}\right]\right.$$
$$\left.\left. + \mathrm{i}\left[\arctan\left(\frac{\epsilon_0^- - k\hbar\Omega}{\Lambda}\right) - \arctan\left(\frac{\epsilon_0}{\Lambda}\right)\right]\right\}\right\}$$
$$+ \frac{\Lambda}{\pi}\sum_{k,p=-\infty}^{\infty}\frac{(-1)^k J_k(\frac{\Delta}{\hbar\Omega})J_p(\frac{\Delta}{\hbar\Omega})}{\omega + (k+p)\Omega}$$
$$\times\left\{\frac{1}{2}\ln\left[\frac{(\epsilon_0^- - p\hbar\Omega)^2 + \Lambda^2}{(\epsilon_0^+ + k\hbar\Omega)^2 + \Lambda^2}\right]\right.$$
$$+ \mathrm{i}\left[\arctan\left(\frac{\epsilon_0^- - p\hbar\Omega}{\Lambda}\right)\right.$$
$$\left.\left. + \arctan\left(\frac{\epsilon_0^+ + k\hbar\Omega}{\Lambda}\right) - \pi\right]\right\} \tag{C.1}$$

at $T = 0$; and at $T > 0$ we have

$$A(\omega) = \mathrm{i}\frac{2\Lambda}{\beta}\sum_{k,p=-\infty}^{\infty}(-1)^{k+1}\frac{J_k(\frac{\Delta}{\hbar\Omega})J_p(\frac{\Delta}{\hbar\Omega})}{\omega + (k+p)\Omega}$$
$$\times\sum_{m=0}^{\infty}\frac{(k-p)\hbar\Omega + 2\epsilon_0}{(\gamma_m + p\hbar\Omega - \epsilon_0^- + \mathrm{i}\Lambda)(\gamma_m + k\hbar\Omega + \epsilon_0^+ + \mathrm{i}\Lambda)}$$
$$+ \mathrm{i}\frac{2\Lambda}{\beta}\sum_{k=-\infty}^{\infty}J_k\left(\frac{\Delta}{\hbar\Omega}\right)$$
$$\times\sum_{m=0}^{\infty}\left[\frac{1}{(\gamma_m + \epsilon_0^+ - k\hbar\Omega + \mathrm{i}\Lambda)(\gamma_m + \epsilon_0 + \mathrm{i}\Lambda)}\right.$$
$$\left. - \frac{1}{(\gamma_m - \epsilon_0^- + k\hbar\Omega + \mathrm{i}\Lambda)(\gamma_m - \epsilon_0 + \mathrm{i}\Lambda)}\right]$$
$$= \frac{\Lambda}{\pi}\sum_{k,p=-\infty}^{\infty}(-1)^{k+1}\frac{J_k(\frac{\Delta}{\hbar\Omega})J_p(\frac{\Delta}{\hbar\Omega})}{\omega + (k+p)\Omega}$$
$$\times\left[\phi\left(\frac{1}{2} + \frac{\Lambda - \mathrm{i}\epsilon_0^+ - \mathrm{i}k\hbar\Omega}{2\pi T}\right)\right.$$
$$\left. - \phi\left(\frac{1}{2} + \frac{\Lambda + \mathrm{i}\epsilon_0^- - \mathrm{i}p\hbar\Omega}{2\pi T}\right)\right]$$
$$+ \frac{\Lambda}{\pi}\sum_{k=-\infty}^{\infty}J_k\left(\frac{\Delta}{\hbar\Omega}\right)\left\{\frac{1}{\omega + k\Omega}\left[\phi\left(\frac{1}{2} + \frac{\Lambda + \mathrm{i}\epsilon_0}{2\pi T}\right)\right.\right.$$
$$\left.\left. + \phi\left(\frac{1}{2} + \frac{\Lambda + \mathrm{i}\epsilon_0^- - \mathrm{i}k\hbar\Omega}{2\pi T}\right)\right] - \frac{1}{\omega - k\Omega}\right.$$
$$\left.\times\left[\phi\left(\frac{1}{2} + \frac{\Lambda - \mathrm{i}\epsilon_0}{2\pi T}\right) - \phi\left(\frac{1}{2} + \frac{\Lambda - \mathrm{i}\epsilon_0^+ + \mathrm{i}k\hbar\Omega}{2\pi T}\right)\right]\right\}. \tag{C.2}$$

References

[1] Aviram A and Ratner M A 1974 *Chem. Phys. Lett.* **29** 277
[2] Datta S 2004 *Nanotechnology* **15** S433
[3] Taylor J, Guo H and Wang J 2001 *Phys. Rev. B* **63** 245407
[4] Xiang J, Lu W, Hu Y, Wu Y, Yan H and Lieber C M 2006 *Nature* **441** 489
[5] Plombon J J, O'Brien K P, Gstrein F, Dubin V M and Jiao Y 2007 *Appl. Phys. Lett.* **90** 063106
[6] Kim Y-H, Tahir-Kheli J, Schultz P A and Goddard W A III 2006 *Phys. Rev. B* **73** 235419
[7] Zheng X, Wang F, Yam C Y, Mo Y and Chen G H 2007 *Phys. Rev. B* **75** 195127
[8] Büttiker M, Thomas H and Prêtre A 1993 *Phys. Lett.* A **180** 364
[9] Nigg S E, López R and Büttiker M 2006 *Phys. Rev. Lett.* **97** 206804
[10] Wang J, Wang B and Guo H 2007 *Phys. Rev. B* **75** 155336
[11] Gabelli J, Fève G, Berroir J M, Placais B, Cavanna A, Etienne B, Jin Y and Glattli D C 2006 *Science* **313** 499
[12] Fu Y and Dudley S C 1993 *Phys. Rev. Lett.* **70** 65
[13] Tu M W Y and Zhang W-M 2008 *Phys. Rev. B* **78** 235311
[14] Prêtre A, Thomas H and Büttiker M 1996 *Phys. Rev. B* **54** 8130
[15] Zheng X, Jin J S and Yan Y J 2008 *New J. Phys.* **10** 093016
[16] Jauho A-P, Wingreen N S and Meir Y 1994 *Phys. Rev. B* **50** 5528
[17] Jin J S, Zheng X and Yan Y J 2008 *J. Chem. Phys.* **128** 234703
[18] Zheng X, Jin J S and Yan Y J 2008 *J. Chem. Phys.* **129** 184112
[19] Zheng X, Luo J Y, Jin J S and Yan Y J 2009 *J. Chem. Phys.* **130** 124508
[20] Zheng X, Jin J S, Welack S, Luo M and Yan Y J 2009 *J. Chem. Phys.* **130** 164708
[21] Keldysh L V 1964 *Zh. Eksp. Teor. Fiz.* **47** 1515
Keldysh L V 1965 *Sov. Phys.—JETP* **20** 1018 (Engl. Transl.)
[22] Stefanucci G and Almbladh C O 2004 *Europhys. Lett.* **67** 14
[23] Polianski M L, Samuelsson P and Büttiker M 2005 *Phys. Rev. B* **72** 161302
[24] Fransson J 2003 *Int. J. Quantum Chem.* **92** 471
[25] Yam C Y, Mo Y, Wang F, Li X, Chen G H, Zheng X, Matsuda Y, Tahir-Kheli J and Goddard W A III 2008 *Nanotechnology* **19** 495203
[26] Yan Y J and Xu R X 2005 *Annu. Rev. Phys. Chem.* **56** 187
[27] Maciejko J, Wang J and Guo H 2006 *Phys. Rev. B* **74** 085324
[28] Stefanucci G and Almbladh C-O 2004 *Phys. Rev. B* **69** 195318
[29] Runge E and Gross E K U 1984 *Phys. Rev. Lett.* **52** 997
[30] Kohn W and Sham L J 1965 *Phys. Rev.* **140** A1133